Temporal trends of plastic additive contents in sediment cores of three French rivers (Loire, Meuse and Moselle) over the last decades

Alice Vidal, Gabrielle Seignemartin, Yoann Copard, Emmanuelle Montargès-Pelletier, Vincent Ollive, Laure Papillon, Christian Grenz, Frédérique Eyrolle, Richard Sempéré

Temporal trends of plastic additive contents in sediment cores of three French rivers (Loire, Meuse and Moselle) over the last decades

Alice Vidal[1], Gabrielle Seignemartin[2], Yoann Copard[3], Emmanuelle Montargès-Pelletier[4], Vincent Ollive[5], Laure Papillon[1], Christian Grenz[1], Frédérique Eyrolle[6], Richard Sempéré[1,7]

[1] Aix-Marseille Univ., Université de Toulon, CNRS, IRD, UM 110, MIO, Marseille, France
[2] Univ. Lyon, Université Claude Bernard Lyon 1, CNRS, ENTPE, UMR5023 LEHNA, F-69518, Vaulx-en-Velin, France
[3] Univ Rouen Normandie, Université Caen Normandie, CNRS, Normandie Univ, M2C UMR 6143, F-76000 Rouen, France
[4] Université de Lorraine, CNRS, Laboratoire Interdisciplinaire des Environnements Continentaux, F-54500 Vandoeuvre les Nancy
[5] Université de Lorraine, Centre de recherche en Géographie, LOTERR, F-54000 Nancy, F-57000 Metz, France
[6] Institut de Radioprotection et de Sureté Nucléaire (IRSN), PSE-ENV, STAAR/LRTA, BP 3, 13115 Saint-Paul-lez-Durance, France
[7] Present address : Aix-Marseille Univ., CNRS, LCE, UM 7376, Ocean Sciences Institute, Marseille, France

Highlights

- Sediment phthalate (PAE) levels were higher than organophosphate ester (OPE) ones.
- PAE and OPE levels increased from the second part of the century until today.
- These increases are likely due to European chemical production at the same period.
- Possible contamination may explain the PAE occurrence in the samples before 1930.
- Tris(2-chloroisopropyl) phosphate (TCPP) was the dominant OPE in sediment cores.
- Di(2-ethylhexyl) phthalate (DEHP) was the dominant PAE in sediment cores.

Abstract

Sediment cores from three major French watersheds (Loire, Meuse and Moselle) have been dated by ^{137}Cs and $^{210}Pb_{xs}$ from 1910 (Loire), 1947 (Meuse) and 1930 (Moselle) until the present in order to reconstruct trajectories of plastic additive contaminants including nine phthalate esters (PAEs) and seven organophosphate esters (OPEs), measured by gas chromatography–mass spectrometer (GC–MS–MS). Historical levels of ∑PAEs were higher than those of ∑OPEs in the Loire and the Moselle sediments, while ∑PAEs and ∑OPEs contents were of the same order of magnitude in the Meuse sediments. Although increases in concentrations do not evolve linearly, our results clearly indicate an increase in OPEs and PAEs concentrations from the 1950-1970 period onwards, compared with the first half of the 20th century. Our results show that, ∑OPE contents increase gradually over time in the Loire and Meuse rivers but evolve more randomly in the Moselle River. Trajectories of ∑PAEs depend on the river and no generality can be established, suggesting sedimentary reworking and/or local contamination. Data from this study allowed comparisons of contents of ∑OPEs and ∑PAEs between rivers, with ∑OPE concentrations in the Moselle River > Meuse River > Loire River, and concentrations of ∑PAEs in the Loire River > Moselle River > Meuse River. Among all PAEs, di(2-ethylhexyl) phthalate (DEHP) was the most abundant in all sediment

samples, followed by diisobutyl phthalate (DiBP). Tris (2-chloroisopropyl) phosphate (TCPP) was the most abundant OPE in sediments of the three rivers. In addition, strong positive Pearson correlations were observed between organic matter (OM) parameters and OPE concentrations, and to a lesser extent, between OM parameters and PAE concentrations. This is particularly true for the Moselle River and for the Loire River, but less so for the Meuse River.

Keywords: Organic plastic additives; Phthalates; Organophosphate esters; River sedimentary archives; Contamination trajectories; Historical pollution

***Abbreviations**:* Tripropyl phosphate (TPP); Tri-iso-butyl phosphate (TiBP); Tributyl-n-phosphate (TnBP); Tris-(2-chloroethyl) phosphate (TCEP); Tris(2-chloro-1-methylethyl) phosphate (TCPP); Tris(chloroisopropyl) phosphate (TCPP-1); Bis(2-chloro-1-methylethyl)(2-chloropropyl) phosphate (TCPP-2); Triphenyl phosphate (TPhP); 2-ethylhexyl diphenyl phosphate (EHDPP); Tri(2-ethylhexyl) phosphate (TEHP); Tris (1,3-dichloro-2-propyl) phosphate (TDCP); Tripropyl phosphate (TPrP); Tricresyl phosphate (TCrP); Tris (1,3-dichloro-2-propyl) phosphate (TDCPP); Tris (2-butoxyethyl) phosphate (TBEP); Diethyl phthalate (DEP); Di(2-ethylhexyl) phthalate (DEHP); Di-n-butyl phthalate (DnBP); Dimethylphthalate (DMP); Diisobutyl phthalate (DiBP); Benzyle butyle phthalate (BBzP); Di-n-octyl phthalate (DnOP).

1. Introduction

Global plastic distribution is at the heart of the environmental concerns of the 21st century, acting as a marker for the Anthropocene. Plastic production has increased exponentially since the nineteen fifties and was estimated at 390.7 million metric tons in 2021 (Statista Research Department, 2023), with most plastic waste being immediately discarded, frequently inappropriately. Some of these objects reach the terrestrial environment and ultimately end up in the aquatic media, in which they become widely distributed (Sonke et al., 2022; Kaandorp et al., 2023). Upon entry into the aquatic compartment, plastics fragment into smaller pieces through photodegradation, weathering, physical abrasion and biotic factors, and can affect ecosystems (Andrady, 2017; Wagner et al., 2018). In addition to environmental concerns caused by global plastic mismanagement, chemicals added to the polymers may be responsible for disrupting ecosystems (Waldschläger et al., 2020). Indeed, thousands of different organic additives are used during plastics manufacturing to give them particular properties (Hermabessiere et al., 2017), and these additives are slowly released into the surrounding environment from plastic debris (Paluselli et al., 2018; Fauvelle et al., 2021). Among plastic additives, phthalates (PAEs) and organophosphate esters (OPEs) are the most abundant (Yang et al., 2019). They are used in various applications: PAEs can be used as plasticizers to facilitate processing and to increase the flexibility and strength of manufactured plastic products, while OPEs can be used as flame retardants and plasticizers, and may be added to paints, adhesives, cosmetics and personal care products (Wang et al., 2020; Guo and Kannan, 2012). In addition, because of their worldwide production and their ubiquity in ecosystems, studies have increasingly focused on their ecotoxicological effects (Net et al., 2015; Wei et al., 2015). However, despite the growing number of scientific studies on occurrence and effects of plastic additives in aquatic ecosystems, knowledge of their spatial and temporal distribution remains limited.

Historical trajectories of contaminants obtained using sediment cores are of great importance, firstly for assessing the emergence of contaminants such as plastic additives, which are transferred by rivers to oceans, and secondly, for evaluating their impacts on the environment over time in relation with 20th century technological and industrial activities. Interestingly, several studies have demonstrated a global accumulation of most PAEs and OPEs in sediments, which can be explained by the strong tendency of these chemicals to bind with carbon-rich suspended particulate matter due to their physicochemical properties, such as their solubility and subsequent accumulation on the sediment floor (van der Veen and de Boer, 2012; Net et al., 2015; Alkan et al., 2021). However, knowledge of historical contamination of OPEs and PAEs in riverine sediments remains limited since most studies either do not date sedimentary archives, or have focused on recent surface sediments. Sedimentary archives from large rivers have been widely explored in Europe in recent years. In France, the Loire, Meuse and Moselle are major rivers hugely impacted by human activities since the beginning of the last century, and their morphology has been strongly modified starting in the 1960s by the construction of dams, wastewater treatment plant inputs and hydro-electrical facilities. Few studies have focused on the presence of microplastics in the Loire River

(Vidal et al. 2023; Dhivert et al. 2022), the Meuse River (Leslie et al. 2017; Hauk et al. 2023) and the Moselle River (Wagner et al. 2014; Utecht and Schuetz 2023), resulting in a lack of data concerning both the isotope-based sedimentary information and the occurrence of plastic additives, such as OPEs and PAEs. To the best of our knowledge, only Castro-Jimenez et al. (2022, SETAC) have presented an exploratory study on the presence of OPEs in sediments and in benthic organisms from the Loire River estuary, and Fromme et al. (2002) have reported limited findings concerning PAEs contents in the Moselle River waters.

The goal of this study was thus to establish the trajectories of the levels of common plastic additives, including seven PAEs and nine OPEs, since the beginning of the last century in dated sediment cores (^{137}Cs and $^{210}Pb_{xs}$) collected at the outlets of the Loire, Meuse and Moselle French watersheds. Parameters related to organic matter (OM) were also measured to establish relationships between these sediment characteristics and the vertical distribution of OPEs and PAEs. These results contribute to a better understanding of plastic additive contamination in freshwater streams and provide data to implement public policies for environmental risk management.

2. Materials and Methods

2.1. Study sites

Core sites were selected in the downstream sections of the Loire, Meuse and Moselle rivers in France (Figure 1-A) by using ancient maps as well as aerial photographs, bibliographic and field investigations to determine areas where sedimentary deposition of fine grain sediments was enhanced, and as far as possible, where yearly floodings were registered in order to converge towards continuity over the last decades.

Geographical context of the Loire core - The Loire River stretches for 1,012 kilometers, covers 117,045 km², and flows into the Atlantic Ocean with an average annual discharge of around 860 $m^3.s^{-1}$ (Tockner et al. 2021). The Loire has been subject to various engineering works that have impacted hydro-sedimentary dynamics, with significant sediment extraction occurring during the second half of the 20th century (Rodriguez et al., 2006) (Figure 1B - Loire). The sediment core was sampled in Montjean-sur-Loire (France) where the drained basin corresponds to 93% (111,172 km²) of the total watershed. It is worth noting that the core is situated just upstream of a weir that deteriorated in the 1980s. Although this weir initially spanned the entire width of the channel, after 1983 it no longer reached the southern bank, potentially altering hydraulic conditions at the core site (Figure S1).

Geographical context of the Meuse core - The Meuse River is 905 kilometers long, covers 34,548 km² and flows into the North Sea with an average annual discharge of around 320 $m^3.s^{-1}$. The Meuse has experienced significant human impact, particularly due to its historical importance as a cross-border river with a densely populated watershed (9 million inhabitants). The core site is at Givet in the upper, French part which covers a drained area of 10,319 km², or 30% of the total watershed. On the east bank of the

Meuse, the core is situated in a reach bypassed by the Canal de l'Est (Northern Branch), a navigation infrastructure dating from the late 19th century (Figure 1B - Meuse).

Geographical context of the Moselle core - The Moselle River, the major tributary of the Rhine River, is 545 km long and exhibits average annual discharge of 315 $m^3.s^{-1}$ with a watershed encompassing approximately 28,133 km². This northern zone is marked by significant industrialization, including steel production, automotive, chemistry, and petrochemicals industries (Wantzen et al., 2022; Le Meur, 2017). The core is situated on the 1956 modified section in France (canalization works). The associated drained area covers about 11,317 km², which is 40% of the entire Moselle watershed. A diachronic series shows that the meander of our study site was reshaped between 1955 and 1966, forming an island (Figure 1B – Moselle). The shift from herbaceous to woody vegetation during this period aligns with decreased hydraulic constraints at the coring site after 1955.

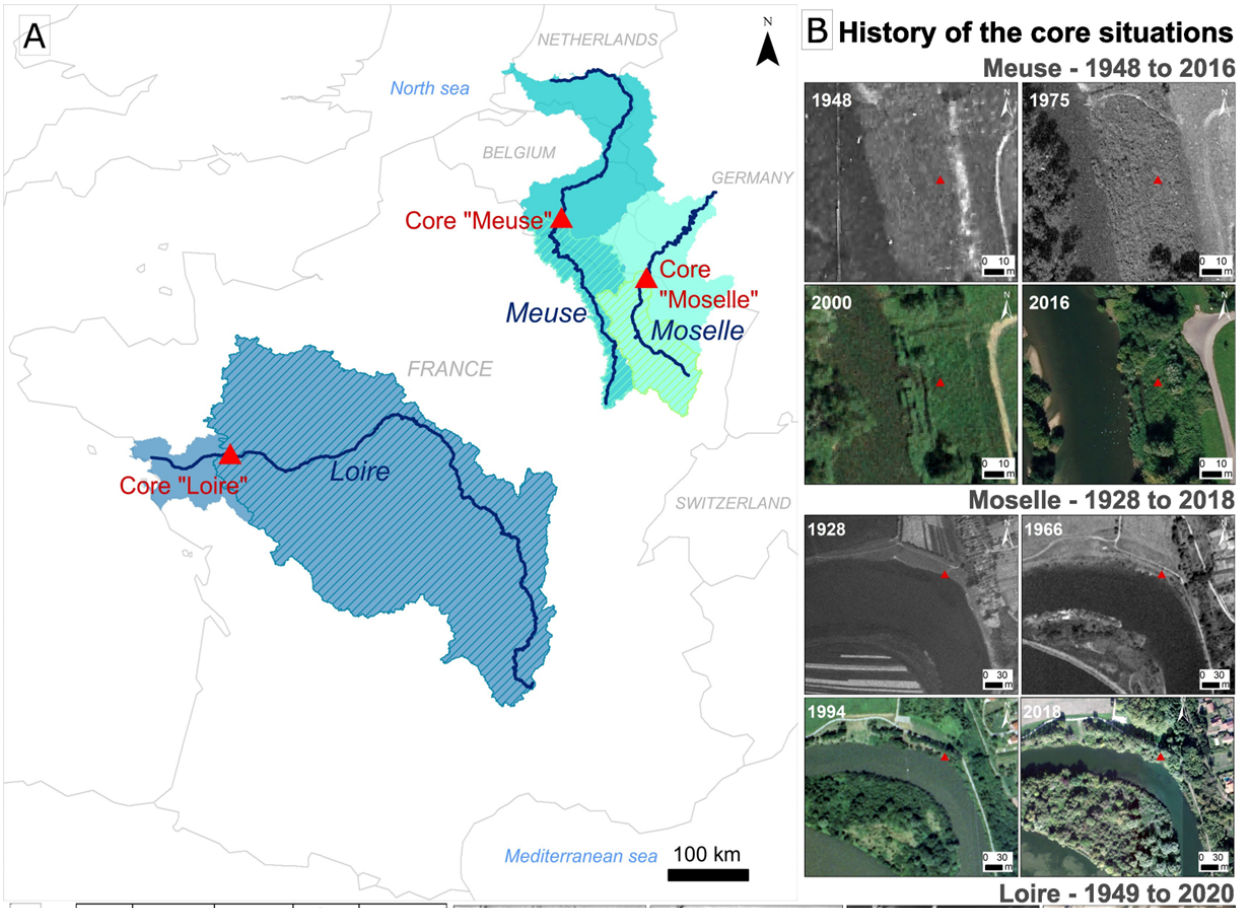

C

	Core length (cm)	Y (WGS 84)	X (WGS 84)	River basin drained at core level (km²)	Percentage of the total river basin (%)
Meuse	82,5	50.152843	4.83322	10,319	31
Moselle	167	49.430889	6.307806	11,317	40
Loire	225	47.392778	-0.856417	111,172	93

Photograph source: IGN, corresponding date

Figure 1. **A.** Location of Loire, Meuse and Moselle cores with associated drained watersheds (shaded); **B.** Historical evolution of coring sites from photographic archives (photograph source: IGN); **C.** Characteristics of the cores.

2.2. Sediment sampling and cores dating

Sediment core samples were collected twice daily on 09/22/2020, 09/29/2021, and 06/28/2022 on the Loire, Moselle and Meuse rivers, respectively, using a percussion driller (Cobra TT, SDEC, France) with transparent PVC tubes (length 1m, diameter 46 mm or 100 mm). The second coring was vertically shifted by 50 cm from the first one in order to preserve sediment samples from interface disruptions. Total core depths ranged from 81 cm for the Meuse River to 167 and 225 cm for the Moselle and Loire Rivers, respectively. Once in the laboratory, each 1 m core was longitudinally cut into slices ranging from 1 to several cm. These were successively sampled, stored at −25°C, then freeze-dried under dehydrated nitrogen flux to avoid any atmospheric exchange, and then sieved at 2 mm before analyses. Sedimentary core samples were analysed by gamma spectrometry to determine the concentration of $^{210}Pb_{xs}$ (^{210}Pb in excess) following (Bouisset and Calmet, 1997; Lefèvre et al., 2003). Around 30% of sedimentary core samples were further analysed by alpha spectrometry after radiochemistry steps in order to quantify plutonium isotopes (^{238}Pu, $^{239,240}Pu$), ^{241}Am and ^{244}Cm. Details of coring sites, core sampling and strata samplings for analyses are described in details in Eyrolle et al. (*submitted*).

^{137}Cs and other chronological tracers dating method (method A) - Sediment core samples were dated using the ^{137}Cs approach consisting in identifying ^{137}Cs enrichment in the sediment cores and correlating these occurrences to peaking atmospheric fallouts, thus allowing to assess sedimentary deposition ages, assuming that post vertical migration due to diffusion or bioturbation mechanisms are restricted. It is of note that the studied rivers are nuclearized and regularly receive low radioactivity liquid effluents such as ^{137}Cs, which partially fix to sedimentary particles and can mask the 1986 Chernobyl accident peak in the sediment cores, depending on the amount released. This can induce complexity in the identification of the 1986 peak, but can also provide additional chronological benchmarks when the radioactive releases chronicles from industries are documented. Additionally, the lack of detection of ^{137}Cs at depth indicates ages pre-dating the bomb tests, i.e. previous to 1955 (Foucher et al., 2021). Artificial alpha emitting radionuclides such as ^{238}Pu, $^{239,240}Pu$, ^{241}Am and ^{244}Cm constitute additional chronological tracers. They, too, peaked in the environment in 1963 due to global atmospheric fallout from nuclear tests, and were regularly released into the Rhone River by the Marcoule spent nuclear fuel reprocessing plant. These releases occurred mainly from 1964 to 1990, at which time this nuclear site began to dismantle, a phase which would last for several decades. Chronological tracers identified along the depth of the core allow to first calculate mean apparent sedimentation rates between two successive benchmarks, and then to determine the age of the sediment core samples by considering that sedimentation rates are constant over the different periods. Uncertainties of age can be estimated from apparent sedimentation rates and from the thickness of sediment slices.

$^{210}Pb_{xs}$ dating method (method B) - Sediment cores were also dated by using Lead-210 isotope as a daughter radionuclide of the ^{238}U radioactive decay series produced by gaseous ^{222}Rn decay. The $^{210}Pb_{xs}$ reaches soils through dry and wet deposition from the atmosphere and is used to date lake sediments where atmospheric inputs are continuous (Appleby, 2008; Foucher et al., 2021). By considering that the

$^{210}Pb_{xs}$ flux is constant, the apparent sedimentary rate can be estimated from the linear regression of the neperian logarithm ln $^{210}Pb_{xs}$ versus depth (Goldberg, 1963):

$$ln(^{210}Pb_{xs}) = ln(^{210}Pb_{0\,xs}) - (\lambda \frac{x}{v})$$

with $^{210}Pb_{0xs}$ the initial $^{210}Pb_{xs}$ at the time of deposit, λ the radioactive decay constant of ^{210}Pb (0.0311 yr^{-1}), x the sediment depth relative to the surface (e.g. cm), and $v=x/t$, the sedimentation rate (e.g. $cm.year^{-1}$). In a system where the initial $^{210}Pb_{xs}$ is constant over time, depth variation of $^{210}Pb_{xs}$ in the sediment column provides the sedimentation rate. This approach requires measuring the activity of ^{210}Pb and of one of its ascendants in radioactive equilibrium with ^{226}Ra. In the present case, as is classically done, the chosen nuclide is ^{214}Bi. The $^{210}Pb_{xs}$ dating method applied onto sedimentary archives collected on alluvial margin is only used in this study to validate method A because this approach can overcome several biases when applied to such sedimentary systems due to (i) variation over time of sedimentary fluxes, (ii) partial remobilisation of sedimentary deposits during floodings, (iii) atmospheric contamination, and (iv) variation with time of the origin of the sedimentary masses.

2.3. Organic matter parameters

Sedimentary Organic Matter (OM) was characterised by using classical bulk organic Rock-Eval 6 pyrolysis (Copard et al., 2006; Baudin et al., 2015), yielding total organic carbon (TOC, in wt.%) content and other OM indicators such as (i) the amount of hydrogenous compounds contained in OM (hydrogen index, in mg hydrocarbon.g^{-1} TOC), (ii) the oxygen index (OI, in mg O_2.g^{-1} TOC) corresponding to the amount of oxygenated compounds contained in OM, and (iii) the residual carbon values (RC, in wt.%) corresponding to the amount of TOC released by the oxidation step (in this study, we specifically used the ratio RC/TOC as an indicator of the importance of the refractory character of OM), and (v) the HI/OI ratio derived from the pyrolysis signals (S2, S3, S3CO), which provides a global origin and the degradation state of OM (Carrie et al., 2012).

2.4. Extraction of OPEs and PAEs

All information on chemical and reagent suppliers is detailed in Table S1. Briefly, sediment samples were sieved through a pre-cleaned stainless-steel sieve (500 µm diameter) before extraction. Our methodology and treatment of sediment samples in the laboratory for PAE and OPE analysis has been previously described in Alkan et al. (2021). Sediments samples (3.00 ± 0.05 g dry weight (dw)) were then mixed with active copper (1 g) and labelled surrogate standards (10 µL of TBP-d27, TCPP-d18, TDCP-d15, DnBP-d4 at 10 $ng.mL^{-1}$) to monitor the overall extraction efficiency of the target compounds. Cartridges (conditioned with acetone, EtOAc and DCM) containing 250 ± 2.5 mg of Oasis MAX (Waters) sandwiched between two PTFE frits were mounted in a 12-port SPE vacuum Manifold (Supelco, Sigma-Aldrich) for the extraction, including three corresponding to blanks for each extraction. Two extractions were undertaken: the first with DCM and the second with DCM/EtOAc (70/30). The combined extracts were evaporated to 1 mL under gentle flow using a 12-port Visidry Drying Attachment (Supelco, Sigma-Aldrich). An additional

clean-up step was performed by passing the extracts through 3% deactivated alumina (1.5 g) packed in a pre-cleaned Pasteur pipette topped with 0.5 g of sodium sulphate. The new extract was then evaporated (50 µL) into a GC vial, and 100 ng of internal standards (TPrP-d21, TCEP-d12, TPhP-d15, DEP-d4 et DEHP-d4) were added to each sample for the quantification of target compounds. Finally, the extracts were stored at −20 °C until Gas Chromatography – tandem Mass Spectrometry (Triple Quadrupole) (GC-MS/MS (QQQ)) analysis.

2.5. Instrumental analysis

GC-MS/MS (QQQ) analyses were conducted with an Agilent 8890 Series GC coupled with an Agilent 7000D TQ, operating in multiple reaction monitoring (MRM) and electron impact (EI, 70 eV) modes (Fauvelle et., 2018). The separation was achieved in a 30 m x 0.25 mm i.d. x 0.25 µm HP-5MS capillary column (Agilent J&W). All target contaminants were quantified by the internal standard (IS) procedure. The injection volume was 2 µL and the helium carrier gas flow was 1 $mL.min^{-1}$. The temperatures of the Mass Selective Detector (MSD) transfer line, the ion source, and the quadrupole were set at 150°C. The following conditions were applied: injector temperature, 270°C (splitless) with the oven programmed from 90°C to 166°C at 4°$C.min^{-1}$, to 175° at 3°$C.min^{-1}$ (holding time 2 min), to 232°C at 4°$C.min^{-1}$, to 290°C at 10°$C.min^{-1}$ and then to 310°C at 10°$C.min^{-1}$ (holding time 7.4 min). The total duration of one sample analysis was 53.45 min.

2.6. Cross-contamination from the coring

Additional analyses were performed to quantify the levels of potential OPEs and PAEs introduced by the PVC made-corer, despite a permanent and rigorous aspiration during the corer cut, and full precautions taken during all the treatment steps. With this aim, an experimental blank sediment sample was baked at 450°C for 6h to eliminate any potential trace of additives and was rewet with ultra-pure water. Blank sediment was introduced into the PVC corer and the same treatment was applied as for the experimental samples. Three replicates of blank sediment were collected at the end of the procedure, were treated to extract the additives (OPEs and PAEs), and then analysed following the same methodology as for the experimental sediment samples. The cross-contamination was quantified for each PAE and each OPE (Table S2). To homogenize the results and allow a comparison between rivers, the given concentrations were first corrected by the recoveries and blank concentrations, and then concentrations from cross-contamination were subtracted.

2.7. Quality assurance/quality control

Strict measures were taken to prevent potential cross contamination during OPE and PAE analysis. First, the use of plastic material was avoided at all times and all glassware was cleaned overnight with detergent, rinsed with tap water + MQ water and then baked at 450°C for 6 h before use. Alumina and sodium sulphate were also baked overnight at 450°C before use. Sample treatment and extraction/clean-up steps were performed entirely in an International Standards Organization (ISO) 6 cleanroom (22°C, SAS + 15 Pa cleanroom pressure, 50 $vol.h^{-1}$ brewing rate) (Paluselli et al., 2018). The retention time and the

response factors of GC-MS/MS (QQQ) were evaluated for each analytical sequence by regularly injecting different calibration levels. One hexane injection was performed every 3 samples to check and monitor potential cross contamination along the sequence. In addition, all samples analysed were spiked with labelled surrogates. The average recoveries and the mean blank values are given for each compound in Table S3. All concentrations of PAE and OPE ($ng.g^{-1}$) presented in this study have been corrected by subtracting the corresponding mean blank value and the concentration due to the coring.

2.8. Statistical analysis

Pearson correlations were performed to evaluate the influence of the organic matter (TOC, RC/TOC, S2, S3, S3CO3 and HI/OI) on plastic additive concentrations over time (PAE and OPE concentrations in sediments of the three rivers). Pearson correlations were performed with the ade4 and FactoMineR packages (Rstudio application associated with R software, version 4.3.1).

3. Results

3.1. Age/depth models based on ^{137}Cs and alpha emitters chronological tracers, and $^{210}Pb_{xs}$ profiles

The ^{137}Cs profile of the Loire River site displays two major peaks at 42.5 and 114.5 cm depth (34.9 $Bq.kg^{-1}$ and 53.3 $Bq.kg^{-1}$, respectively), and ^{137}Cs is no longer detected below 134.5 cm. ^{241}Am also peaks at 114.5 cm depth, signifying the period of atmospheric global fallout from nuclear tests (Figure 2A). The later ^{137}Cs peaks are attributed to 1986 (Chernobyl civil nuclear accident) and 1963 (Atmospheric global fallout from nuclear tests), respectively. The sandy strata observed at 134.5-139.5 cm and again at 162.5, 188 and 202 cm depth may be related to the major successive floods that occurred between 1953 and 1955 for the upper sedimentary strata, then between 1941 and 1945 for the deepest ones, as suggested by Morereau (2020), while the last thick sandy stratum at 222.5 cm depth is associated to 1910 (Figure S2). The 1910 flood was the most important hydrological event, lasting 2 months and contributing to 55% of the annual water flow in 1910–1911 (Grosbois et al., 2012). Owing to these chronological benchmarks, determined apparent sediment rate (ARS) ranged from 0.9 $cm.y^{-1}$ for the 1910-1941 period to a maximum of 9.9 $cm.y^{-1}$ for the 1941-1945 period, including the sandy deposits of the floods (Figure 2C). Since 1945, ARSs reveal intermediate values estimated at 1.6 $cm.y^{-1}$ for the more recent period (1986-2020), and at 3.3 $cm.y^{-1}$ for the 1963-1986 period (Figure 2C). As mentioned in previous studies performed on the same coring site, the $^{210}Pb_{xs}$ profile displays negative values, mostly due to excess ^{226}Ra from unknown origin, and cannot, therefore, be used to support results obtained from method A (Figure 2B, D).

Four benchmarks were retained for the Meuse core including 62, 42, 29 and 19 cm depth corresponding to the first detection of ^{137}Cs (1955), as well as the three ^{137}Cs peaks (Figure 2E). The ^{137}Cs peak at 29 cm depth is attributed to the 1971 accidental release from the Chooz nuclear power plant (NPPs), while the two others are associated with the years 1963 and 1986. In 1971, the ^{137}Cs annual releases from the Chooz NPPs was around ten times higher than in both the previous and the following years, suggesting that this event was significantly imprinted within the studied sediment core. The

detection of ^{241}Am close to the ^{137}Cs peak at 42 cm depth attributed to 1963 validates the origin of this peak (Figure 2E). Based on these chronological benchmarks, the estimated ARSs are 2.5, 1.6, 0.7 and 0.5 $cm.y^{-1}$ for the successive periods 1955-1963, 1963-1971, 1972-1986 and 1986-2021, respectively (Figure 2G). Method B, applied from the surface to 42 cm depth where stable $^{210}Pb_{xs}$ contents are reached, gives an ARS of 0.6 $cm.y^{-1}$, which is in line with the values determined using method A (Figures 2F and 2H).

Rising ^{137}Cs activities start at 112.5 cm depth for the Moselle core within fine grain sediments deposited above the thick sandy stratum observed in the deepest layers of the core, i.e., below 127 cm depth (Figure 2I and Figure S2). The layer at 112.5 cm depth is then associated to 1955, while the ^{137}Cs peaks signaling the global atmospheric fallout from nuclear tests and the Chernobyl accident are placed at 49.8 and 25 cm depth, respectively. Disrupted profiles of both ^{137}Cs, ^{241}Am and $^{210}Pb_{xs}$ between 112.5 and 30 cm depth most probably highlight a discontinued sedimentation, due either to a partial remobilization of previously deposited sediments before bank stabilization, or to sediment inputs from varying origins (Figures 2I and 2J). The emergence of a small island at the end of the 1950, due to the Moselle canalization, may explain disruption (Figure 1.B–Moselle). Finally, reconstruction of floods using data recorded at the Uckange hydrometric station - around 35 km upstream of the coring site and in operation since 1981 - and archive data for older heights indicate an extreme flood in 1947. The thick sandy layer below 127 cm can be associated to this major hydrological event. From these chronological benchmarks, ARSs of 1.8, 7.8, 1.1 and 0.7 $cm.y^{-1}$ are associated to the successive periods 1947-1955, 1955-1963, 1963-1986, and 1986-2021 (Figure 2K). Method B validates the age of the core with a mean ARS of 1.7 $cm.y^{-1}$ for the entire period 1947-2021 (Figure 2L).

For the three rivers, age/depth models based on method A were used to convert core depth to years (Figure 2).

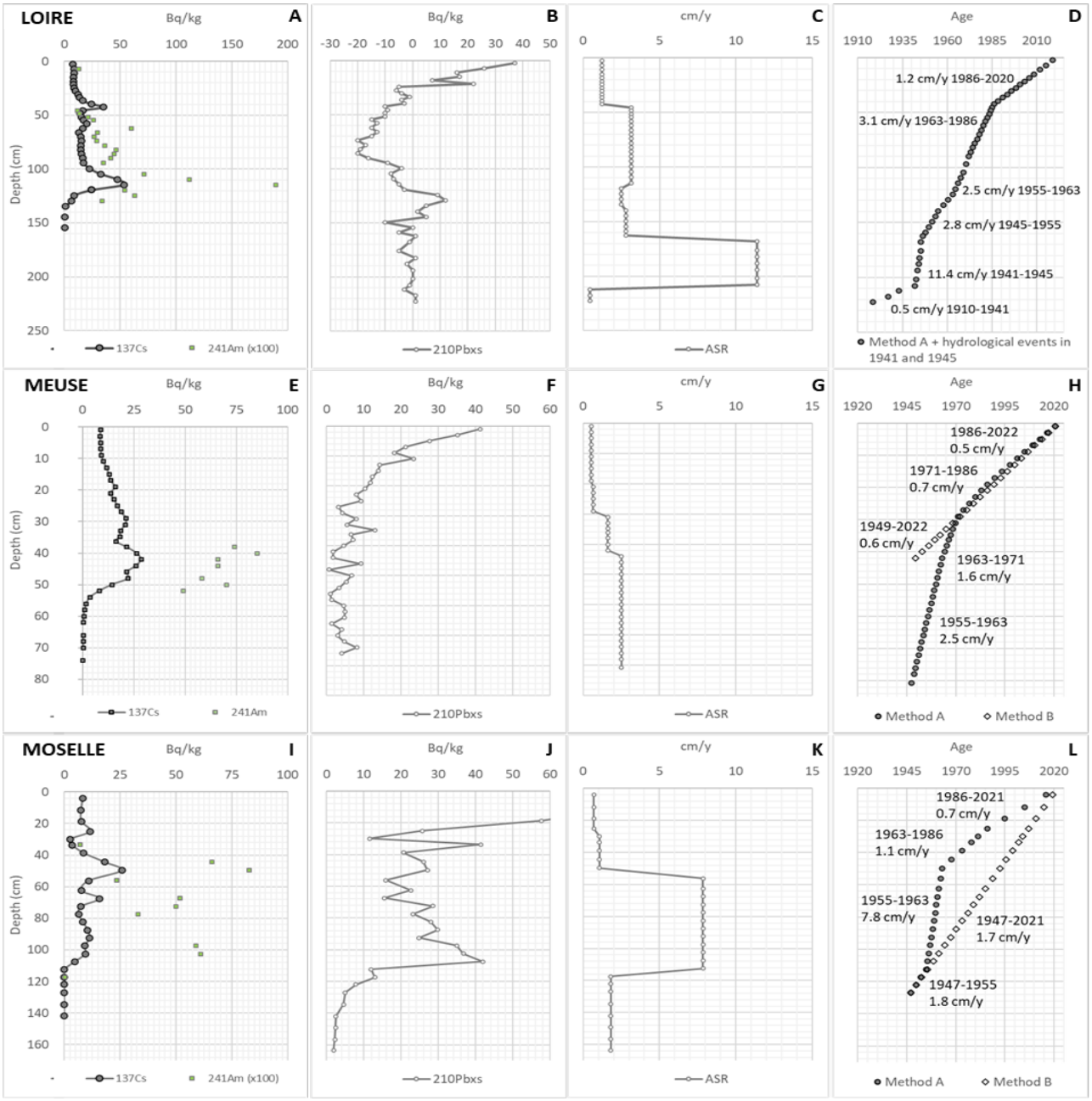

Figure 2. Profiles along the depth (cm) of ^{137}Cs and ^{241}Am (A, E, I), $^{210}Pb_{xs}$ (B, F, J) (Bq.kg^{-1}, at the time of sampling), Apparent Sedimentation Rate (ARS, in cm.y^{-1}) (C, G, K) and estimated age using Method A (^{137}Cs) and Method B ($^{210}Pb_{xs}$) (D, H, L) for the Loire (A, B, C, D), Meuse (E, F, G, H) and Moselle (I, J, K, L) sediment cores.

3.2 Organic matter parameters

Our results show that TOC content decreased with depth, from 5.10% to 0.24% for the Loire River and from 5.80% to 0.36% for the Moselle River, with a lesser decrease observed for the Meuse River (4.48%-2.39%). In the Meuse River, the highest value was reported in year 1947.5 (Table 1). The RC/TOC ratio values were roughly similar for the three rivers, ranging from 0.68 to 0.87 (Table 1). Values of S2, S3, S3CO and HI/OI differed depending on the river (Table 1).

Table 1. Organic carbon total (TOC, wt. %), ratio of residual carbon to organic carbon total (RC/TOC), hydrocarbons (S2, S3, S3CO), and the ratio of the index of hydrogen over the index of oxygen (HI/OI) for the Loire, Meuse and Moselle sediment samples.

Year	Depth (cm)	TOC (%)	RC/ TOC	S2	S3CO	S3	HI/OI
Loire							
2018.7	**2.5**	5.10	0.71	13.23	2.29	8.53	1.76
2015.0	**7.0**	4.33	0.73	10.42	2.06	7.47	1.58
2011.8	**11.0**	3.67	0.73	8.37	1.81	6.46	1.46
2008.5	**15.0**	3.31	0.73	7.44	1.65	5.91	1.42
2005.6	**18.5**	3.02	0.74	6.56	1.51	5.41	1.37
2000.7	**24.5**	2.43	0.74	5.16	1.26	4.67	1.25
1995.8	**30.5**	2.18	0.76	4.26	1.16	4.04	1.18
1988.5	**39.5**	2.11	0.76	4.07	1.11	3.85	1.19
1977.8	**70.0**	1.86	0.77	3.20	1.00	3.50	1.03
1963.0	**119.5**	2.64	0.83	3.42	1.12	3.95	0.98
1960.3	**124.5**	3.84	0.87	3.84	1.10	3.76	1.14
1957.7	**129.5**	3.59	0.86	3.96	1.06	3.48	1.26
1949.6	**149.5**	1.57	0.86	1.48	0.58	2.41	0.71
1931.9	**208.0**	1.43	0.86	1.56	0.45	1.61	1.09
1910.0	**222.5**	0.24	0.83	0.28	0.08	0.36	0.91
Meuse							
2021.2	**1.0**	4.41	0.73	9.40	2.20	10.21	0.92
2016.7	**3.0**	3.74	0.73	7.99	1.74	8.23	0.97
2012.9	**5.0**	3.50	0.74	6.95	1.65	7.89	0.88
2009.1	**7.0**	3.08	0.75	5.90	1.44	7.08	0.83
2005.2	**9.0**	3.11	0.73	6.39	1.47	7.51	0.85
2001.4	**11.0**	2.79	0.75	5.40	1.29	6.33	0.85
1997.5	**13.0**	2.63	0.76	4.80	1.25	5.91	0.81
1989.8	**17.0**	2.40	0.76	4.21	1.15	5.76	0.73
1977.0	**42.0**	2.46	0.77	3.90	1.17	6.25	0.63
1963.0	**46.0**	2.39	0.79	3.45	0.98	5.38	0.64
1960.6	**58.0**	2.82	0.79	4.03	1.16	6.91	0.58
1955.0	**62.0**	3.37	0.86	3.18	0.92	5.55	0.57
1947.5	**80.0**	4.48	0.83	5.84	1.25	6.53	0.89
Moselle							
2016.0	**4.5**	5.80	0.68	17.07	2.61	9.92	1.96
2004.9	**13.4**	8.81	0.68	26.80	3.80	13.21	2.27
1994.9	**21.3**	5.17	0.71	13.85	2.24	6.99	2.18
1981.4	**34.1**	2.29	0.79	4.47	0.55	1.78	2.77
1977.9	**38.4**	3.22	0.69	10.16	0.87	3.38	3.43
1967.9	**50.6**	3.91	0.74	10.24	0.90	3.91	3.05
1961.3	**71.0**	3.48	0.81	5.15	1.24	5.06	1.17
1957.5	**105.1**	5.28	0.85	6.44	1.24	5.37	1.39
1956.2	**116.5**	4.57	0.78	9.37	1.28	5.49	1.99
1955.0	**127.8**	3.13	0.79	5.24	1.26	4.71	1.26
1947.0	**144.3**	1.25	0.80	1.90	0.59	1.95	1.09
1938.7	**161.4**	0.28	0.71	0.74	0.08	0.48	1.87
1930.6	**178.1**	0.36	0.78	0.53	0.18	0.83	0.75

3.3. Environmental levels of PAEs and OPEs in Loire, Meuse and Moselle sediments

Our results show that globally, both OPEs and PAEs concentrations were higher after 1950 than before, although slight PAE decreases were observed near the surface in the period 1980-2020 (Figure 3). Sediment samples from the Loire and the Moselle rivers present higher concentrations of ∑PAEs than of OPEs, whereas these additive levels were quite similar in the Meuse sediments (Figure 3). In the Loire River, PAEs were detected since the first record in 1910 (Figure 3B), while OPEs first appeared in 1955 (Figure 3A). In the Meuse and the Moselle rivers, OPEs and PAEs were detected from the first records (1947.5 and 1930.6, respectively). However, levels of PAEs were higher than OPEs at the earliest dates (Figures 3C, 3D, 3E and 3F). It must be noted that contamination cannot be ruled out for such compounds in our sediment core

samples (during sampling and storage steps). OPE contents in the Loire and in the Meuse rivers have progressively increased (Figures 3A and 3C). By contrast, we observed three distinct contamination periods in the Moselle sediments: pre-1955, between 1955 and 1967.9, and post-1967.9 (Figure 3E). In addition, the highest concentrations of ∑OPEs were measured in the Moselle River and the lowest were measured in the Loire River. However, the highest concentrations of PAEs were measured in the Loire River and the lowest in the Meuse River. PAE levels increase gradually over time in the Loire River sediments, but they vary more randomly in the Meuse and the Moselle rivers. In the Meuse River, concentrations are seen to fluctuate between 15 and 50 ng g^{-1} dw depending on the year, and to peak intermittently in the Moselle River, in 1930.6, 1955.6 and 1977.9.

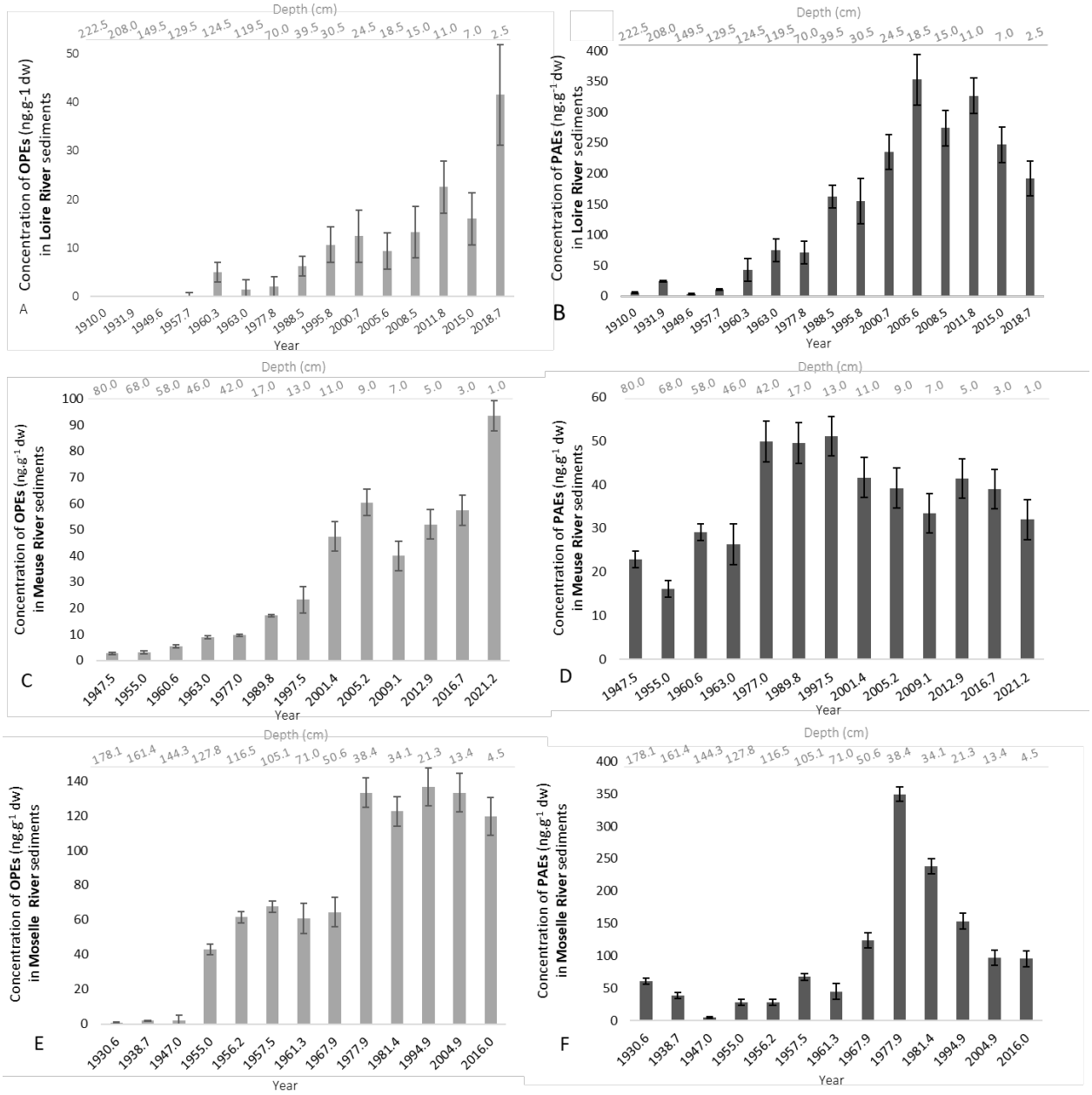

Figure 3. Environmental levels (ng.g^{-1} dw) of OPEs (A, C and E) and PAEs (B, D and F) by year and depth, measured in the sediment of the Loire River (A and B), the Meuse River (C and D) and the Moselle River (E and F).

3.5. Relative abundances of PAEs and OPEs in sediments of the Loire, Meuse and Moselle rivers

In sediments of the three rivers, TCPP was the dominant OPE and DEHP was the dominant PAE (Figures 4; Tables S4, S5, S6). In the Meuse and the Moselle rivers, no presence of TPP and TnBP was detected, while all the other PAEs were measured at least once (Figures 4C, 4D, 4E and 4F). The profile of the targeted additives in the Loire River is unusual, since TPP and TiBP were not detected at all, and neither were DMP, DEP nor DnOP (Figure 4A and 4B), unlike in the other two rivers. Figures 4B, 4D and 4F show the decreasing contribution of DiBP and DnBP over time in all rivers, and particularly apparent in the Loire River, at the expense of an increasing contribution of DEHP which appeared for the first time in 1963 in the Loire and in the Meuse rivers, and earlier in the Moselle River, in 1930.

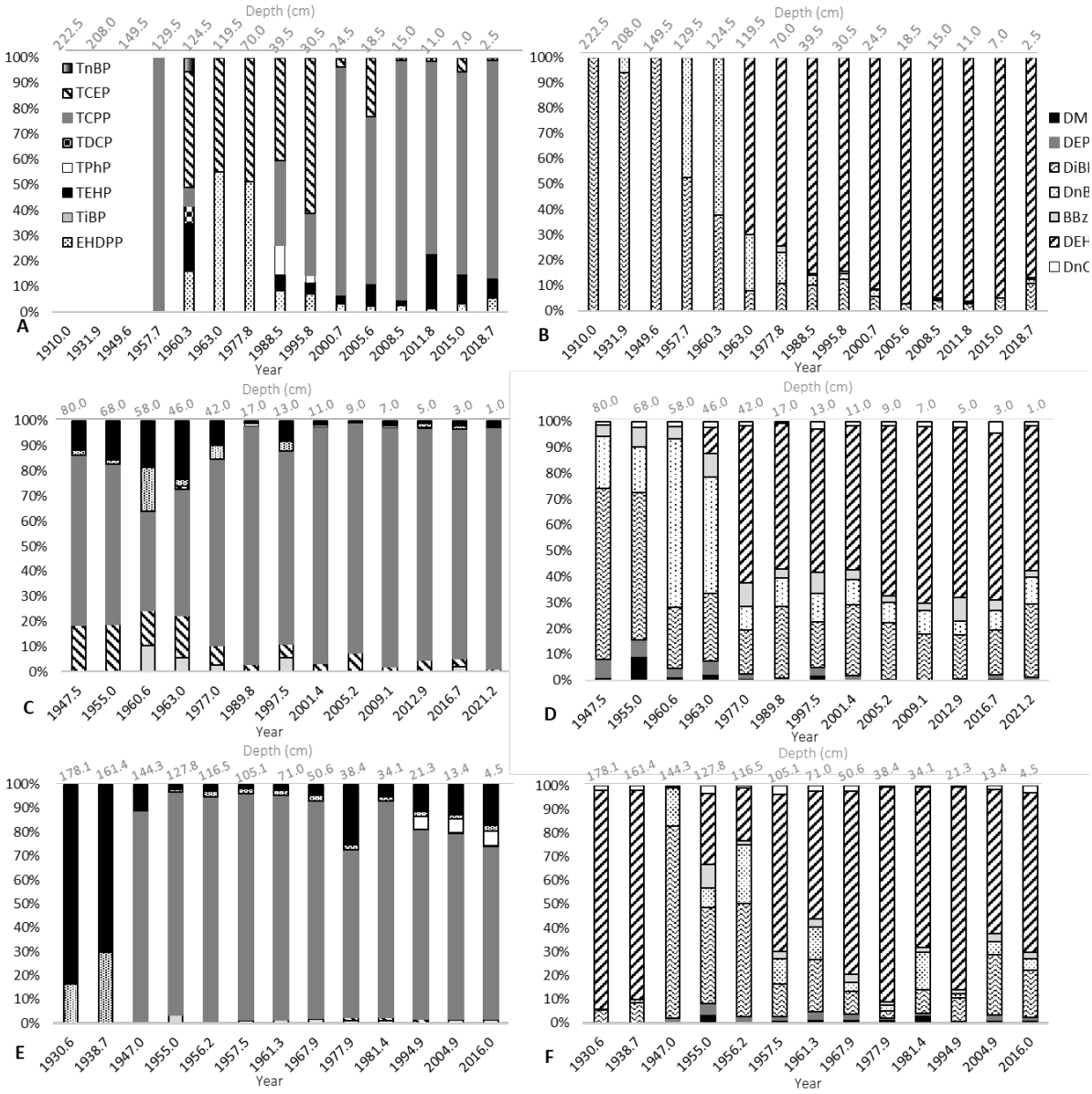

Figure 4. Relative abundances of individual OPE (A, C and E) and PAE (B, D and F) measured in the sediment of the Loire River (A and B), the Meuse River (C and D) and the Moselle River (E and F).

3.5. Relationship between plastic additive levels and organic matter

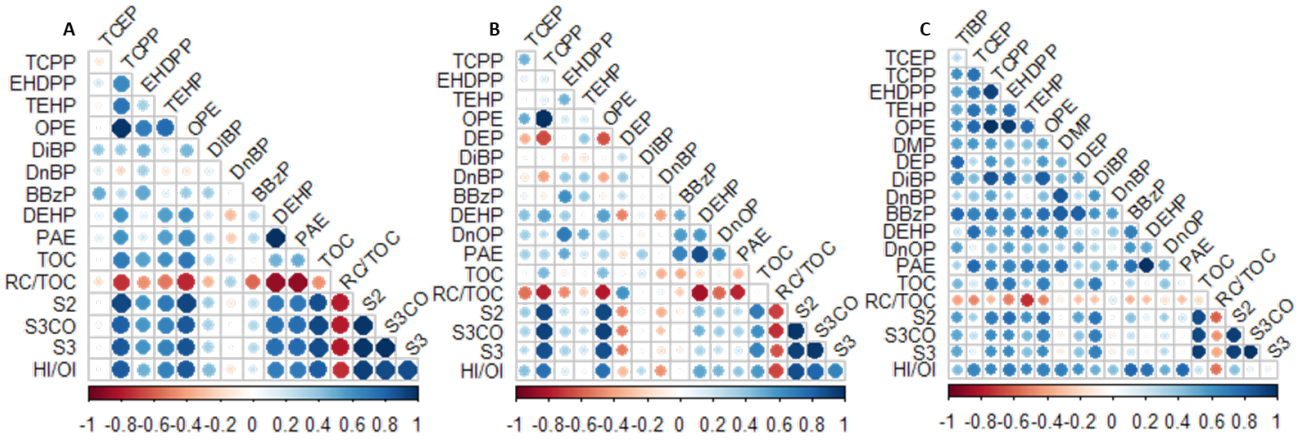

Figure 5. Pearson correlations of the levels of chemicals (individual OPE, total OPEs, individual PAE, total PAEs) and all organic matter factors (TOC, RC/TOC, S2, S3, S3CO and HI/OI ratio), for the Loire (A), the Meuse (B) and the Moselle (C). The red circles correspond to anti-correlations while the blue ones correspond to correlations. The larger the diameter of the circles, the stronger the correlations.

Figure 5 shows that in general, levels of individual OPE, total OPEs, individual PAE, and total PAEs are positively correlated to values of TOC, S2, S3CO, S3 and HI/OI, and negatively correlated to values of RC/TOC. More correlations were observed in the Moselle River (Figure 5C), while only a few results were reported in the Meuse River (Figure 5B). In general, OPEs (individual and total) show stronger correlations with OM parameters than do PAEs. In all sediment cores from the rivers studied, TCEP shows low correlations with OM parameters, while TCPP is strongly correlated to these parameters. In the Loire (Figure 5A) and the Moselle (Figure 5C) rivers, TEHP and EHDPP show relatively strong correlations with OM, but this is not the case in the Meuse River. This also applies for DEP, which presents positive correlations with OM in the Moselle River but negative ones in the Meuse River. Levels of DiBP, DnBP and BBzP seem not to depend on OM in any of the three rivers. Finally, DEHP distribution is strongly correlated with OM parameters in the Loire River, but not in the two other rivers.

4. Discussion

Despite PAEs and OPEs being commonly encountered in aquatic media, information on their historical contamination in freshwaters is limited, since only a few studies have investigated and dated sediment cores. Data on additive production volume during the earlier years is not available at the scale of the studied watersheds but van der Veen and de Boer (2012) demonstrated that OPEs have been employed worldwide for up to 150 years and that PAEs have been used since the beginning of the 20th century. Today, OPEs and PAEs are in the class of synthetic chemicals with high production volumes and toxicological properties (Schecter et al. 2013). Establishing the trajectories of plastic additives in sediment archives may therefore contribute to the reconstructions of environmental and human exposures to these contaminants that have been made over the last decades. In this study, we focus on three major rivers: the Loire River is the longest river in France, and the Meuse and Moselle rivers cross several NW European countries, yet to the best of our knowledge, no data on plastic additive historical pollution are available in the literature. Nevertheless, we can notice that significant PAE and OPE increases could be associated

to the plastic and various chemical production reported for the second part of the 20th century. It is important to note that PAEs and OPEs concentrations are significantly lower in the Moselle and Loire rivers. The Meuse River, is flowing through France, Belgium and Netherlands and is associated with both industrial and agricultural activities along its course, though the prevalence of each can vary by region. Indeed, in its upper reaches within France, the Meuse flows through regions that have historically been more rural and agricultural. The Loire and the Moselle are two more populated regions and with greater industrial development (for example the steel industry for the Moselle). An in-depth sociological and economic study would be relevant to explain the contamination of sediments with OPEs and PAEs in a more local way, but it is extremely difficult to provide it at the watersheds scale.

Temporal trends of OPE and PAE levels. Results of this study show that OPEs and PAEs in the Loire, the Meuse and the Moselle sediment cores are present since the earliest dates recorded (1910, 1947.5 and 1930.6, respectively). Several studies have measured levels of PAEs and OPEs for decades. For example, Kang et al. (2016) showed historical contamination of some PAEs, dating DiBP and DnBP in Lake Chaohu (China) sediments to 1849, and Cao et al. (2017), who investigated the contamination of OPEs in sediment cores from Lake Michigan (USA), reported concentrations of alkyl- and chlorinated -OPEs since 1860. The increasing vertical concentrations of plastic additives over time in the Loire, Meuse and Moselle rivers indicate ongoing contamination by both OPEs and PAEs. These results are consistent with the history of these plastic additives. PAEs have been the most commonly used plasticizers in a variety of industrial and consumer products for more than 80 years (Net et al., 2015, Li et al. 2017), and OPEs were first introduced in the early 1900s, with their use increasing rapidly after the 1940s (USEPA, 1976). In 2009, worldwide PAE production stood at 6.2 million tons (He et al., 2019), of which a large portion is likely to be found in aquatic ecosystems, and in 2018, 1.05 million tons of OPEs were used globally (Z.C. Group, 2018), subsequent to the ban on polybrominated diphenyl ethers (Stapleton et al., 2012). Kim et al. (2021) further investigated the influence of industries and populations in an attempt to explain the fate of PAEs in aquatic ecosystems, and found that temporal trends for PAE concentrations in a sediment core were significantly correlated with the numbers of industrial facilities and with increasing populations. This suggests that industrialization and anthropogenic activities are major influencing factors in PAE contamination. Similarly, higher concentration of OPEs and PAEs have been also reported in anthropized areas compared to protected areas in Mediterranean coastal surface sediment (Alkan et al., 2021).

In this study, we report that the respective contamination trends of OPEs and PAEs are different. Indeed, OPE contents have increased gradually over the years, while PAEs values show intermittent peaks, suggesting either periodic and localised historical pollution events, a variability of sedimentary deposits and possible contamination of sediment core samples. These results might be explained by the various sources and uses of these chemicals, and by their different fates in the environment. Furthermore, among all PAEs measured in this study, DEHP was dominant, followed by DiBP. Kim et al. (2021) also detected PAEs in each sediment core collected in Korea's industrialized Ulsan and Onsan bays, with concentrations

of DEHP ranging from 33.4 to 30,000 (median: 600) $ng.g^{-1}$ dw, making it the dominant PAE. Previous studies also reported DEHP as the dominant PAE in sediment samples, ranging from 42% to 72% of ΣPAE concentrations (Alkan et al., 2021; Chen et al., 2017; Li et al., 2017). This can be explained not only by the high use of DEHP in industries, but also by its greater persistence in the environment. Indeed, in aquatic media, the high molecular weight PAEs are preferentially adsorbed on particles due to a higher hydrophobicity, as shown by a high octanol-water partitioning coefficient (Kow) (Kim et al., 2021; Lee et al., 2019). Alternatively, DEHP is also very abundant in the atmosphere, so material and sample contamination of this molecule cannot be excluded. In addition, Kim et al. (2021) observed the highest concentrations of PAEs in sediment from rivers compared to streams and inner parts of bays, suggesting that proximity to industrial complexes is crucial for sedimentary distribution of plasticizers. Among all OPEs, TCPP was predominant in sediments of the three rivers, which is consistent with previous studies. For example, Zhang et al. (2018) found that TCPP accounted for 35% of the total OPEs measured in coastal beaches in China, and Ma et al. (2022) found that TCPP had an average contribution of 81% in sediments of the Dong Nai River (Vietnam). TCPP is an extensively produced flame retardant worldwide and is added to polymers but does not chemically bind to them, facilitating its release into the environment through volatilization, abrasion, dissolution, and through direct contact with particle surfaces (Rauert et al., 2014), which may explain its ubiquity.

Relationship between plastic additive contents and organic matter

To unravel the factors governing historical trends of plastic additives, we performed Pearson correlations between concentrations of PAEs, concentrations of OPEs and organic matter parameters (Figure 5). Published studies on this topic remain rare and there is no consensus on reported results. Herein, positive and significant correlations between plastic additive contents and OM parameters are seen to occur essentially with pyrolyzed C (S2, S3, S3CO), while the negative correlations occur with refractory C (RC/TOC). Accordingly, the adsorption mechanism may concern the labile fraction of sedimentary OM which exhibits chemical functional groups such as CH_2, CH_3 (e.g methyl) for hydrogen and COH, CO (alcohol, ketone, ester) for oxygen. In general, correlations were stronger in the case of OPEs than PAEs, suggesting that OM might be more influential in the fate of OPEs than in that of PAEs. Kim et al. (2021) also reported that TOC was not an influencing factor in the distribution of PAEs in sedimentary environments. However, Chen et al. (2018) showed that OM may play a key role in DEHP distribution in the sediments during the dry season, whereas DEHP concentrations in the wet season may be principally affected by other environmental and hydrological conditions (transport, mixing and sedimentation mechanisms). In our study, DEHP concentrations were correlated with OM parameters in the case of the Loire River but to a lesser extent for the Meuse and the Moselle rivers. Kang et al. (2016) also highlighted the significantly positive relationship between TOC and ΣPAEs levels, as well as low-molecular-weight PAEs (DMP, DEP, DIBP, DnBP, DEHP). This result was not corroborated by our findings, and nor did we find a correlation between concentrations of these molecules and OM. Concerning the distribution of the OPEs,

Ma et al. (2022) showed that the concentrations of TCPP and TEHP exhibit a significant moderate positive correlation with TOC. Zhao et al. (2023) reported weak but positive Spearman correlations between TOC and ∑OPEs (i.e., TEHP, TCEP, TPhP) in fishing port sediments (Dalian, North China). OPEs with low water solubility such as TEHP, EHDPP, TPhP, TnBP and TiBP are preferentially adsorbed onto particulate OM (Martínez-Carballo et al., 2007). Compounds with higher logKow or higher logKoc values were more easily adsorbed onto sediment constituents, while OPEs with logKoc > 5 were almost completely associated with sediment particles (Cao et al., 2017; Ma et al., 2022). Despite the wide variability in hydrophobicity of the targeted OPEs, specific interactions or common migration pathways between polar functional groups of TOC and OPEs may contribute to the observed relationships and may partially explain OPE distributions (Zhao et al., 2023). Research on the parameters influencing plastic additive distribution is still limited and further studies are needed for enhanced understanding. The additives studied here are potentially degradable in sediment, as are the rest of the organic compounds, but very probably with different kinetics. It is important to note that the presence of contaminants such as OPEs can also induce a decrease in the diversity of the bacterial community (such as the number of microbial species), as has been demonstrated for OPEs in coastal Mediterranean marine sediments (Castro-Jiménez et al., 2022b). This modification may very likely influence the degradation kinetics of natural organic matter.

5. Conclusion

The contents of ∑9OPEs and ∑7PAEs have increased overall in the three studied rivers since they were first detected in sediment deposits, i.e. since 1910 for the Loire River, 1947 for the Meuse River and 1930 for the Moselle River. The contents of OPEs has increased progressively over time, while trajectories of PAEs are not linear. The results of this study highlight the environmental changes that occurred during this industrial period and show how riverine sediments provide a useful record for reporting environmental impacts related to human activities. Our data are helpful for an improved understanding of the fate of these chemicals in freshwater compartments and for establishing relationships between contamination in sedimentary archives and anthropogenic pressures. Finally, our results will contribute towards a better protection of aquatic media and the development of a management strategy concerning plastic additives.

Acknowledgements

The authors are grateful to the ANR TRAJECTOIRE project (ANR-19-CE3- 0009) 2020–2024 for financial support and partly to ANR RIOMAR project under the France 2030 (ANR 22 POCE 0006), and warmly thank Benoit Losson (Université de Lorraine, Centre de recherche en Géographie, LOTERR), Claire Delus (LOTERR) and Laurence Mansuy-Huault (LIEC), who participated in the initial identification and sample coring. We also thank Brice Mourier, Thierry Winiarsky (Univ. Lyon. Université Claude Bernard Lyon 1. CNRS. ENTPE. UMR5023 LEHNA), Hugo Lepage, Valérie Nicoulaud-Gouin, Franck Giner, David Mourier, Xavier Cagnat and Anne De Vismes (Institut de Radioprotection et de Sureté Nucléaire (IRSN), Maxime

491 Chastanet and Alexandra Coynel (EPOC, Bordeau), François Baudin (ISTeP laboratory, Sorbonne Université
492 for RE6 analyses) for their help during field work and sample analyses.

493

References

Alkan, N., Alkan, A., Castro-Jiménez, J., Royer, F., Papillon, L., Ourgaud, M., Sempéré, R., 2021. Environmental occurrence of phthalate and organophosphate esters in sediments across the Gulf of Lion (NW Mediterranean Sea). Sci. Total Environ. 760, 143412. https://doi.org/10.1016/j.scitotenv.2020.143412

Andrady, A.L. 2017. The plastic in microplastics: A review. Marine Pollution Bulletin. 119, 12-22. https://doi.org/10.1016/j.marpolbul.2017.01.082.

Baudin, F., Disnar, J.-R., Aboussou, A., Savignac, F. 2015. Guidelines for Rock–Eval analysis of recent marine sediments. Organic Geochemistry. 86, 71–80. https://doi.org/10.1016/j.orggeochem.2015.06.009

Bouisset, P., Calmet, D. 1997. Hyper pure gamma-ray spectrometry applied to low-level environmental sample measurements. International Workshop on the Status of Measurement Techniques for the Identification of Nuclear Signatures, Geel, Belgium.

Cao, D., Guo, J., Wang, Y., Li, Z., Liang, K., Corcoran, M. B., et al. 2017. Organophosphate esters in sediment of the great lakes. Environ. Sci. Technol. 51, 1441–1449. https://doi.org/10.1021/acs.est.6b05484

Carrie, J., Sanei, H., Stern, G. 2012. Standardisation of Rock–Eval pyrolysis for the analysis of recent sediments and soils. Organic Geochemistry. 46, 38–53. https://doi.org/10.1016/j.orggeochem.2012.01.011

Castro-Jimenez, J., Aminot, Y., Pollono, C., Idjaton, B., Bizzozero, L. et al. 2022. Environmental occurrence of organophosphate esters and micro-plastics in sediments and benthic organisms from the Loire Estuary (France). SETAC Europe 32nd Annual Meeting, COPENHAGUE, Denmark. SETAC Europe 32nd Annual Meeting, 1p., 2022.

Castro-Jiménez, J., Cuny, P., Militon, C. et al. 2022b. Effective degradation of organophosphate ester flame retardants and plasticizers in coastal sediments under high urban pressure. Sci Rep 12, 20228. https://doi.org/10.1038/s41598-022-24685-6

Chen, C.F., Chen, C.W., Ju, Y.R., Dong, C.D., 2017. Determination and assessment of phthalate esters content in sediments from Kaohsiung Harbor, Taiwan. Mar. Pollut. Bull. 124, 767–774.

Chen, C.F., Ju, Y.R., Lim, Y.C., Chang, J.H., Chen, C.W., Dong, C.D. 2018. Spatial and Temporal Distribution of Di-(2-ethylhexyl) Phthalate in Urban River Sediments. Int J Environ Res Public Health. 11, 15-2228. https://doi.org/10.3390/ijerph15102228

Copard, Y., Di-Giovanni, C., Martaud, T., Albéric, P., & Olivier, J.E. 2006. Using Rock-Eval 6 pyrolysis for tracking fossil organic carbon in modern environments: implications for the roles of erosion and weathering. Earth Surface Processes and Landforms. 31, 135–153. https://doi.org/10.1002/esp.1319

Dendievel, A.M., Grosbois, C., Ayrault, S., Evrard, O., Coynel, A., Debret, M., Gardes, T., Euzen, C., Schmitt, L., Chabaux, F., Winiarski, T., Van Der Perk, M., Mourier, B. 2022. Key factors influencing metal concentrations in sediments along Western European Rivers: A long-term monitoring study (1945–2020). Science of The Total Environment 805. 149778. https://doi.org/10.1016/j.scitotenv.2021.149778

Dhivert, E., Phuong, N.N., Mourier, B., Grosbois, C., Gasperi, J. 2022. Microplastic trapping in dam reservoirs driven by complex hydrosedimentary processes (Villerest Reservoir, Loire River, France). Water Res. 15, 225-119187. https://doi.org/10.1016/j.watres.2022.119187

Dhivert, E., Phuong, N.N., Mourier, B., Grosbois, C., Gasperi, J. 2022. Microplastic trapping in dam reservoirs driven by complex hydrosedimentary processes (Villerest Reservoir, Loire River, France). Water Research. 225, 0043-1354. https://doi.org/10.1016/j.watres.2022.119187

Eyrolle, F., Boyer P., Chaboche P-A., De Vismes A., Lepage H., Seignemartin G., Mourier B., Evrard O., et al. Temporal trajectories of artificial radiocaesium 137Cs in French rivers over the nuclear era reconstructed from sediment cores, Scientific reports, *submitted*.

Fauvelle, V., Castro-Jiménez, J., Carlez, B., Schmidt, N., Sempéré, R. 2018. One-single extraction procedure for the simultaneous determination of a wide range of polar and non-polar organic contaminants in marine surface water. Front. Mar. Sci. 5:295. https://doi.org/10.3389/fmars.2018.00295.

Fauvelle, V., Garel, M., Tamburini, C. et al. 2021. Organic additive release from plastic to seawater is lower under deep-sea conditions. Nat Commun 12, 4426. https://doi.org/10.1038/s41467-021-24738-w

Fromme, H., Küchler, T., Otto, T., Pilz, K., Müller, J., Wenzel, A. 2002. Occurrence of phthalates and bisphenol A and F in the environment. Water Res 36, 1429–1438.

Grosbois, C., Meybeck, M., Lestel, L., Lefèvre, I., Moatar, F., 2012. Severe and contrasted polymetallic contamination patterns (1900–2009) in the Loire River sediments (France). Science of The Total Environment 435–436, 290–305. https://doi.org/10.1016/j.scitotenv.2012.06.056

Guo, Y. and Kannan, K. 2012. Challenges Encountered in the Analysis of Phthalate Esters in Foodstuffs and Other Biological Matrices. Analytical and Bioanalytical Chemistry; 404, 2539–2554. https://doi.org/10.1007/s00216-012-5999-2

Hauk, R., van Emmerik, T.H.M, van der Ploeg, M., de Winter, W., Boonstra, M., Löhr, A.J., Teuling A.J. 2023. Macroplastic deposition and flushing in the Meuse River following the July 2021 European floods. Environmental Research Letters. 18, 124025. https://doi.org/10.1088/1748-9326/ad0768

He, Y., Wang, Q., He, W., Xu, F., 2019. The occurrence, composition and partitioning of phthalate esters (PAEs) in the water-suspended particulate matter (SPM) system of Lake. Sci. Total Environ. 661, 285-293. https://doi.org/10.1016/j.scitotenv.2019.01.161

Hermabessiere, L., Dehaut, A., Paul-Pont, I., Lacroix, C., Jezequel, R., Soudant, P., Duflos, G. 2017. Occurrence and effects of plastic additives on marine environments and organisms: A review. Chemosphere. 182, 781-793. https://doi.org/10.1016/j.chemosphere.2017.05.096

Kaandorp, M.L.A., Lobelle, D., Kehl, C. et al. 2023. Global mass of buoyant marine plastics dominated by large long-lived debris. Nat. Geosci. 16, 689–694. https://doi.org/10.1038/s41561-023-01216-0

Kang, L., Wang, QM., He, QS. et al. 2016. Current status and historical variations of phthalate ester (PAE) contamination in the sediments from a large Chinese lake (Lake Chaohu). Environ Sci Pollut Res. 23, 10393–10405. https://doi.org/10.1007/s11356-015-5173-4

Kim, S., Kim, Y., Moon, H.B. 2021. Contamination and historical trends of legacy and emerging plasticizers in sediment from highly industrialized bays of Korea. Science of The Total Environment. 765, 142751. https://doi.org/10.1016/j.scitotenv.2020.142751

Le Meur, M., Mansuy-Huault, L., Lorgeoux, C., Bauer, AL, Gley, R., Vantelon, D., Montargès-Pelletier, E. 2017. Spatial and temporal variations of particulate organic matter from Moselle River and tributaries: A multimolecular investigation. Organic Geochemistry. 110, 45-56. https://doi.org/10.1016/j.orggeochem.2017.04.003

Lee, Y.S., Lee, S., Lim, J.E., Moon, H.B. 2019. Occurrence and emission of phthalates and non-phthalate plasticizers in sludge from wastewater treatment plants in Korea. Sci. Total Environ. 692, 354–360.

Lefèvre, O., Bouisset, P., Germain, P., Barker, E., Kerlau, G., Cagnat, X. 2003. Self-absorption correction factor applied to 129I measurement by direct gamma–X spectrometry for Fucus serratus samples. Nuclear Instruments and Methods in Physics Research A. 506, 173–185.

Leslie, H.A., Brandsma, S.H., van Velzen, M.J., Vethaak, A.D. 2017. Microplastics en route: Field measurements in the Dutch river delta and Amsterdam canals, wastewater treatment plants, North Sea sediments and biota. Environ Int. 101, 133-142. https://doi.org/10.1016/j.envint.2017.01.018

Li, R., Liang, J., Gong, Z., Zhang, N., Duan, H., 2017. Occurrence, spatial distribution, historical trend and ecological risk of phthalate esters in the Jiulong River, Southeast China. Sci. Total Environ. 580, 388–397.

Ma, Y., Saito, Y., Ta, T.K.O., Li, Y., Yao, Q., Yang, C., Nguyen, V. L., Gugliotta, M., Wang, Z., Chen, L. 2022. Distribution of organophosphate esters influenced by human activities and fluvial-tidal interactions in the Dong Nai River System, Vietnam. Science of The Total Environment. 812, 152649.

Morereau, A., 2020. Reconstitution à partir d'archives sédimentaires des concentrations et des sources des radionucléides ayant transité dans le Rhône et la Loire au cours de l'ère nucléaire (Thèse de doctorat). Aix-Marseille Université

Net, S., Sempéré, R., Delmont, A., Paluselli, A., Ouddane, B. 2015. Occurrence, fate and behavior and ecotoxicological state of phthalates in different environmental matrices. Environ. Sci. Technol. 49, 4019–4035. https://doi.org/10.1021/es505233b

Paluselli A, Fauvelle V, Galgani F, Sempéré R. 2019. Phthalate Release from Plastic Fragments and Degradation in Seawater. Environ Sci Technol. 53:166-175. https://doi.org/10.1021/acs.est.8b05083

Rauert, C., Lazarov, B., Harrad, S., Covaci, A., Stranger, M. 2014. A review of chamber experiments for determining specific emission rates and investigating migration pathways of flame retardants. Atmos Environ. 82, 44–55. https://doi.org/10.1016/j.atmosenv.2013.10.003

Rodrigues, S., Bréhéret, J.G., Macaire, J.J., Moatar, F., Nistoran, D., Jugé, P. 2006. Flow and sediment dynamics in the vegetated secondary channels of an anabranching river: The Loire River (France). Sedimentary Geology. 186, 89-109. https://doi.org/10.1016/j.sedgeo.2005.11.011.

Schecter, A., Lorber, M., Guo, Y., Wu, Q., Yun, H.S., Kannan, K., Hommel, M., Imran, N.S.L., Cheng, D.H., Colacino, J.A., Birnbaum, L.S. 2013. Phthalate concentrations and dietary exposure from food purchased in New York state. Environ. Health Perspect. 121, 473–479.

Sonke, J.E., Koenig, A.M., Yakovenko, N. et al. 2022. A mass budget and box model of global plastics cycling, degradation and dispersal in the land-ocean-atmosphere system. Micropl.&Nanopl. 2, 28. https://doi.org/10.1186/s43591-022-00048-w

Stapleton, H. M., Sharma, S., Getzinger, G., Ferguson, P.L., Gabriel, M., Webster, T.F., Blum, A. 2012. Novel and high volume use flame retardants in US couches reflective of the 2005 pentaBDE phase out. Environ. Sci. Technol. 46, 13432−13439.

Statista Research Department, Jun 12, 2023. https://www.statista.com/statistics/282732/global-production-of-plastics-since-1950/

Tockner, K., Zarfl, C., Robinson, C.T. 2021. Rivers of Europe - 2nd Edition. 2nd edition. ed. Elsevier.

USEPA. 1986. EPA Regulation 40 CFR part 136 (appendix b) appendix b to part 136 d definition and procedure for the determination of the method detection limited revision 1.11 (US Environmental Protection Agency (EPA). Available at: http://www.ecfr.gov/(Accessed 5 March 2013).

Utecht, S. and Schuetz, T. 2023. A depth-resolved snapshot of microplastic abundances in riffle heads in a gravelbed river, EGU General Assembly 2023, Vienna, Austria, 24–28 Apr 2023, EGU23-673, https://doi.org/10.5194/egusphere-egu23-673, 2023

van der Veen, I. and de Boer, J. 2012. Phosphorus flame retardants: properties, production environmental occurrence, toxicity and analysis. Chemosphere 88, 1119–1153. https://doi.org/10.1016/j.chemosphere.2012.03.067

Vidal, A., Phuong, N.N., Métais, I., Gasperi, J., Châtel, A. 2023. Assessment of microplastic contamination in the Loire River (France) throughout analysis of different biotic and abiotic freshwater matrices. Environ Pollut. 1, 334:122167. https://doi.org/10.1016/j.envpol.2023.122167

Wagner, M., Scherer, C., Alvarez-Muñoz, D., Brennholt, N., Bourrain, X., Buchinger, S., Fries, E., Grosbois, C., Klasmeier, J., Marti, T., Rodriguez-Mozaz, S., Urbatzka, R., Vethaak, A.D., Winther-Nielsen, M., Reifferscheid, G. 2014. Microplastics in freshwater ecosystems: what we know and what we need to know. Environ Sci Eur. 26(1):12. https://doi.org/10.1186/s12302-014-0012-7

Wagner, M., Lambert, S. (Eds.), 2018. Freshwater Microplastics: Emerging Environmental Contaminants?, The Handbook of Environmental Chemistry. Springer International Publishing, Cham. https://doi.org/10.1007/978-3-319-61615-5

Waldschläger, K., Lechthaler, S., Stauch, G., Schüttrumpf, H., 2020. The way of microplastic through the environment – Application of the source-pathway-receptor model (review). Science of The Total Environment 713, 136584. https://doi.org/10.1016/j.scitotenv.2020.136584

Wang, X., Zhu, Q.Q., Yan, X.T., Wang, Y.W., Liao, C.Y., and Jiang, G.B. 2020. A review of organophosphate flame retardants and plasticizers in the environment: Analysis, occurrence and risk assessment. Sci. Total Environ. 731, 139071. https://www.10.1016/j.scitotenv.2020.139071

Wantzen, K.M., Uehlinger, U., Van der Velde, G., Leuven, R.S.E.W., Schmitt, L., Beisel, J.N., 2022. Chapter 10 - The Rhine River basin. in: Tockner. K. Zarfl. C. Robinson. C.T. (Eds.). Rivers of Europe (Second Edition). Elsevier. pp. 333–391. https://doi.org/10.1016/B978-0-08-102612-0.00010-9

Wei, G.L., Li, D.Q., Zhuo, M.N., Liao, Y.S., Xie, Z.Y., Guo, T.L., Li, J.J., Zhang, S.Y., Liang, Z.Q. 2015. Organophosphorus flame retardants and plasticizers: sources, occurrence, toxicity and human exposure. Environ. Pollut. 196, 29–46. https://doi.org/10.1016/j.envpol.2014.09.012

Yang, J., Zhao, Y., Li, M., Du, M., Li, X., Li, Y., 2019. A review of a class of emerging contaminants: the classification, distribution, intensity of consumption, synthesis routes, environmental effects and expectation of pollution abatement to organophosphate flame retardants (OPFRs). Int. J. Mol. Sci. 20, 1–38. https://doi.org/10.3390/ijms20122874

Z.C. Group, In-depth Investigation and Investment Prospect Analysis Report of China's Flame Retardant Market in 2014–2018, Zhiyan Consulting Group, 2018.

651 Zhang, H., Zhou, Q., Xie, Z., Zhou, Y., Tu, C., Fu, C., Mi, W., Ebinghaus, R., Christie, P., Luo, Y. 2018.
652 Occurrences of organophosphorus esters and phthalates in the microplastics from the coastal beaches
653 in north China. Sci Total Environ. 616-617:1505-1512. https://doi.org/10.1016/j.scitotenv.2017.10.163
654 Zhao, S., Liu, X., Wu, Z., Lin, T., Sun, H., Wang, W., Guo, Z., Yao, Z. 2023. Investigating the presence of
655 organophosphate esters in sediments from a typical fishing port agglomeration in Dalian, North China.
656 Environmental Pollution. 334, 0269-7491. https://doi.org/10.1016/j.envpol.2023.122233.
657